Naval Research Laboratory

Washington, DC 20375-5320

NRL/MR/7220--02-8617

Optical Refraction Measurements Across Chesapeake Bay

LEE U. MARTIN

Computational Physics, Inc.
Springfield, VA

WILLIAM P. HOOPER

Remote Sensing Physics Branch
Remote Sensing Division

April 30, 2002

REPORT DOCUMENTATION PAGE

Form Approved
OMB No. 0704-0188

1. REPORT DATE *(DD-MM-YYYY)*	2. REPORT TYPE	3. DATES COVERED *(From - To)*
April 30, 2002	Memorandum Report	01 October 1999-1 March 2002

4. TITLE AND SUBTITLE

Optical Refraction Measurements Across Chesapeake Bay

5a. CONTRACT NUMBER

5b. GRANT NUMBER

5c. PROGRAM ELEMENT NUMBER

6. AUTHOR(S)

Lee U. Martin* and William P. Hooper

5d. PROJECT NUMBER

5e. TASK NUMBER

5f. WORK UNIT NUMBER

7. PERFORMING ORGANIZATION NAME(S) AND ADDRESS(ES)

Naval Research Laboratory
Washington, DC 20375-5320

8. PERFORMING ORGANIZATION REPORT NUMBER

NRL/MR/7220--02-8617

9. SPONSORING / MONITORING AGENCY NAME(S) AND ADDRESS(ES)

Office of Naval Research
800 North Quincy Street
Arlington, VA 22217

10. SPONSOR / MONITOR'S ACRONYM(S)

11. SPONSOR / MONITOR'S REPORT NUMBER(S)

12. DISTRIBUTION / AVAILABILITY STATEMENT

Approved for public release; distribution is unlimited.

13. SUPPLEMENTARY NOTES

*Computational Physics, Inc., Springfield, VA

14. ABSTRACT

The refraction of light was measured across a 16.2 km over-water path across Chesapeake Bay in order to recover the low-level temperature profiles. The apparent elevation of buoys and lights on a tower are observed from a number of different heights (ranging from 3 m to 30 m). This report describes the refractive measurements, the statistics of over 500 observations and their relationship to the observed meteorological conditions taken over an 18-month period. An analysis of refraction under stable and unstable conditions is discussed and a non-dimensional approach for displaying the results is shown. In addition, a technique for monitoring the height variations of the water surface is discussed.

15. SUBJECT TERMS

Refraction, Mirage, Temperature gradient

16. SECURITY CLASSIFICATION OF:			17. LIMITATION OF ABSTRACT	18. NUMBER OF PAGES	19a. NAME OF RESPONSIBLE PERSON
a. REPORT	b. ABSTRACT	c. THIS PAGE			William P. Hooper
Unclassified	Unclassified	Unclassified	UL	23	19b. TELEPHONE NUMBER *(include area code)* (202) 767-3317

Standard Form 298 (Rev. 8-98)
Prescribed by ANSI Std. Z39.18

CONTENTS

OPTICAL REFRACTION MEASUREMENTS ACROSS CHESAPEAKE BAY

1. INTRODUCTION

As is well known and documented (Ref. 1,2), light is bent by the temperature gradient of the medium through which light rays pass. In theory (Ref. 3-6), it is possible to reconstruct the temperature profile from the amount of bending. To this end, a preliminary study was conceived and conducted to measure the bending of light rays in order to recover the temperature profiles above a water surface. The ultimate goal is to develop the technique for use with a shipboard lidar. This report describes the measurements of the refraction, the statistics of the refractive data and the relationships to the meteorological conditions at the time. The recovery of temperature profiles from the refractive data is written up in a paper titled "Retrieval of Near-Surface Temperatures Profiles from Passive and Active Optical Measurements"(Ref. 7).

2. MEASUREMENT PROCEDURES

The investigation measured the day-to-day changes in elevation angle to lights mounted on a tower across a 16.2 kilometer over-water path. The investigation was conducted between the Naval Research Laboratory's (NRL's) field research facilities at Chesapeake Bay Detachment (CBD) and Tilghman Island. CBD, at 38.67 N and 76.53 W, is located near Chesapeake Beach, 40 miles southeast of Washington D.C., on the western shore of Chesapeake Bay. Tilghman Island is directly across the Bay on the eastern shore, a distance of 16.2 km. (see Fig.1).

The angles were measured with a commercial surveying station (Pentax Model PTS-V2). It has a 32X magnification telescope whose angle accuracy, i.e. standard deviation, is 2 seconds of arc. At a range of 16.2 km, this gives an accuracy of 0.156 meters.

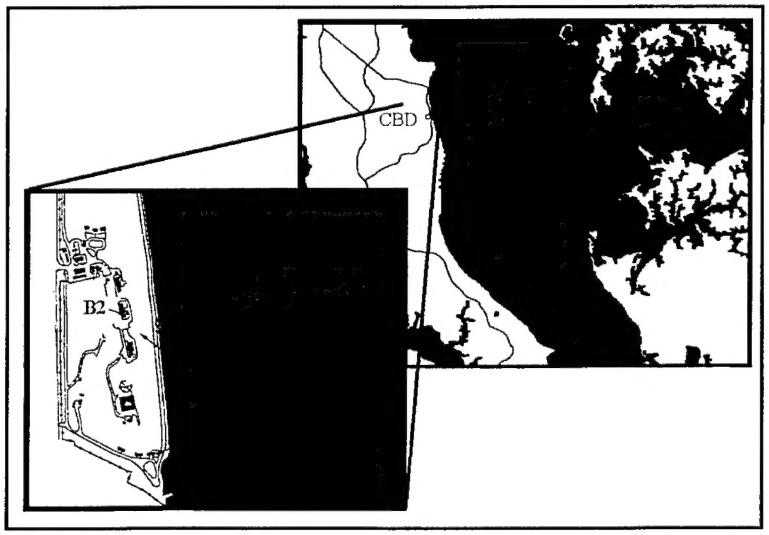

Figure 1

Manuscript submitted March 19, 2002.

The lights were 1500 watt quartz construction lights mounted on a 27 m (90 feet) tower, see figure 2. Two lights were initially installed at heights of 4.7 m (15.4 feet) and 24.4 m (80 feet) above mean water level. Later, two more lights were added at intermediate heights of 9.5 m (31.1 feet) and 13.7 m (45 feet). To increase their lifetime, they were turned on and off near sunrise and sunset respectively by timers. Measurements were taken twice a day, near sunrise and mid-day, five days a week for a period of about 18 months. To increase angle accuracy, an average of five observations of each light's position were noted.

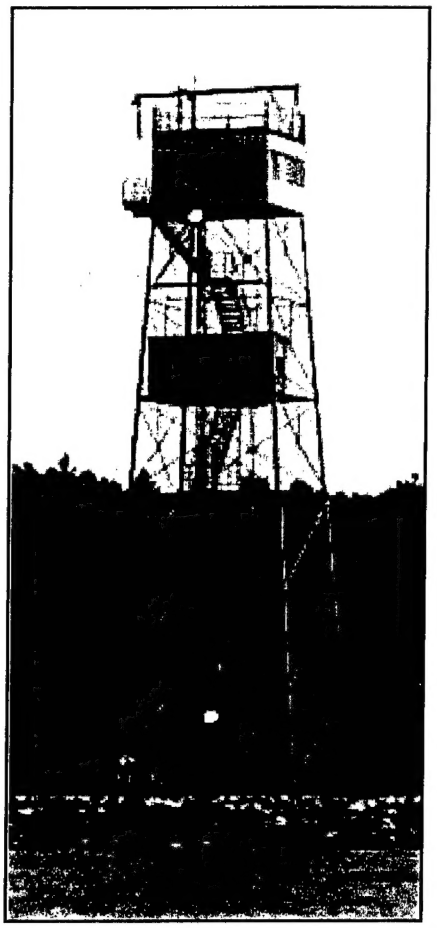

Figure 2

Observing sites at CBD varied during the time of the investigation. Two of the sites (the second lowest and highest) have remained in use the entire time, while other sites have been added and dropped. Figure 3 shows the second lowest site in use. Observing heights were 2.3 (Bw), 3.5 (P), 5.4 (Pl), 12.7 (H), 27.7 (C) and 37 m (B2) above mean water level (see Fig. 1 insert with corresponding letters). The sites were not co-located because of the terrain geometry at CBD, which consists of a narrow shoreline in front of a steep cliff . Consequently, the sites ranged from the top of the breakwater at the shoreline (hgt = 2.3 m) to a second story room in a building on top of the cliff (hgt = 37 m). Three of the sites were close to the water level, one was at an intermediate height, one at the cliff-top itself and the highest in a building on top of the cliff.

Figure 3

Since the amount of bending of the light rays depends upon the low-level temperature profile, supporting ground truth data were important. Ground truth for the measurements came from several sources, although all of them were not ultimately useful. Air and water temperatures were routinely measured concurrently with the angle data. These data were acquired from the end of a 125 meter pier that extends out into the Bay from the shoreline at CBD. However,

during some weather situations, these data were not considered representative of the over-water conditions between sites. This occurred during times of warm land temperatures and off-shore winds.

However, air and water temperatures over the Bay were available from two other sources. One was from a buoy located near the middle of the Bay approximately 12.3 miles south of the line-of-site path between the sites. This buoy, which will be called mid-bay buoy or MBB, is one of several that are part of the Chesapeake Bay Observing system run by several local universities (William and Mary College, Univ. of Maryland, Old Dominion Univ.). These buoys provide real-time continuous meteorological and oceanographic data from various locations around the Bay. The data are recorded every half-hour and are available on their Internet site at www.cbos.org. These data were available except during times of data transmission problems, routine maintenance and/or removal of the buoys if the Bay would freeze during the winter.

The second source was from a lighthouse, Thomas Point, that is part of the National Data Buoy Center's (NDBC) collection of platforms (buoys, towers, etc.) operated by the National Oceanographic and Atmospheric Administration (NOAA). It is located 13.6 miles north of the line-of-sight path approximately mid-way across the Bay. It has more sensors than the mid-bay buoy, but records only hourly meteorological data. The air temperature data is from a height of 17.4 meters, too high for direct comparison to the mid-bay buoy, who's height was estimated at 3 meters. However, the temperature data were used with the mid-bay buoy data to construct vertical temperature profiles that proved to be useful in the data analysis. These data are also listed on the Internet at www.ndbc.noaa.gov and are routinely available, except for occasional maintenance and sensor problems.

The mid-bay buoy provided the bulk of the ground-truth data for the observations. However, these data were supplemented on several occasions by measurements from a landing craft used as part of the investigation (see Ref. 7). Temperature and humidity data were collected from seven R. M. Young temperature/humidity sensors mounted on a tower and a structure that extended from the bow of the vessel toward the water. This configuration provided profiles from 0.5 to 20 meters above the surface. Disadvantages of this approach included the short-term nature of the data and contamination of the lowest sensor during high wave conditions. In addition to the environmental data, lights identical to those on the tower were mounted on the landing craft. Several days of data were acquired measuring the angles to these lights as the vessel moved across the Bay, thereby monitoring refractivity changes as a function of range.

3. DATA DESCRIPTION AND ANALYSIS

As mentioned previously, the data consisted of elevation angles to the lights taken from the various survey points. Data were available except when conditions were unfavorable. These included not only the usual rain, snow, etc., but during times of high winds and extremes of atmospheric stability, both stable and unstable.

High winds generated large waves and turbulence, either blocking the lower light from view and/or smearing the lights together. This was especially true from the lowest sites. Similarly, strong unstable conditions would spread the lights out along the tower, making one continuous light. These effects could be minimized in future experiments by either separating the lights further apart in the horizontal direction or remotely turning on and off individual lights. In contrast, during stable conditions, haze would often form over the water between the sites, reducing visibility to the point that the lights were not observable.

Before giving specific examples of the results, the general behavior of the data will be described. The number of lights observed, their position, separation and the presence of images varied with time, depending upon atmospheric stability. The amount of variation depended upon the height of the observing site, with the greatest variations occurring for the lowest heights, where the temperature gradients were strongest.

During slight to moderately stable conditions, all of the lights were visible, small in diameter and didn't fluctuate in position. This was true, even from the lowest site, as long as the conditions were not too hazy. Stable profiles produce less downward bending of the light rays, so the lights appeared at a higher elevation angle, see figure 4a (ray trajectories) and 4b (tower image). This allowed all of the lights to be observed across the 16.2 km path.

As the atmosphere became less stable, i.e. close to neutral stability, the rays were bent more toward the earth, striking the water surface. Consequently, the lowest light disappeared from view, leaving only the upper lights and the water surface (i.e. the horizon) visible.

As the conditions became more unstable, the horizon decreased further in angle and an image of the upper light appeared, see figure 4c (ray trajectories) and 4d (tower image). In this case, there were two paths for the light rays to travel to the observer, a direct path and one that skims the surface and is bent back up toward the observer. This lower ray makes it appear that the image is below the astronomical horizon (ie. below zero degree elevation). The light and it's image are separated by the caustic, which is the point in space dividing the upright scene from it's

inverted image. Under strongly unstable conditions, the rays from the lower light bend up and the lower light can no longer be seen from by the survey station when it is located at a lower observation location.

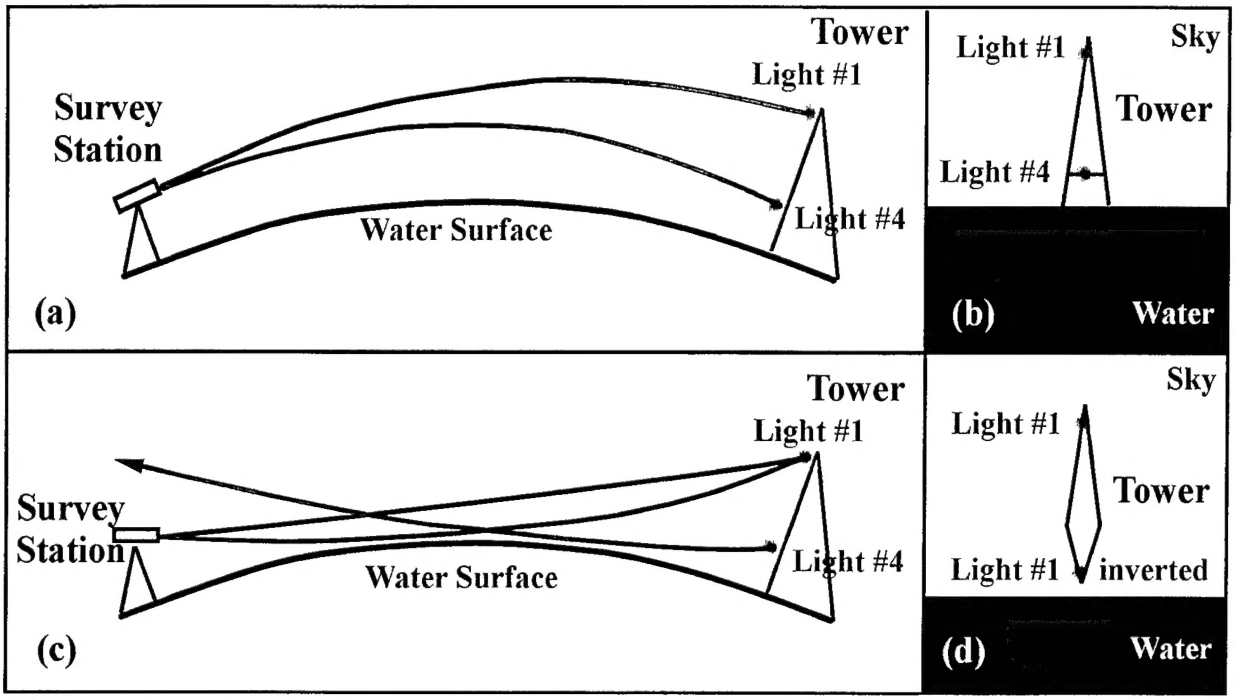

Figure 4

The appearance of images is dependent upon the height of the observing site, with images of the upper light occurring most often at the lowest survey point. This is where the strongest temperature gradients occur most frequently. However, the greatest number of images were observed at 12.7 meters, where one would occasionally see images of three of the four lights.

Additionally during unstable conditions, the lights expanded in diameter and fluctuated in position, depending upon the instability, wind speed and direction. Under strongly unstable conditions, the lights appeared flame-like, growing and shrinking over time intervals of seconds. Overall, the results changed with the seasons, with more unstable cases occurring during the fall and stable cases during the spring.

Figure 5a shows the distribution of temperature gradients observed at the mid-bay buoy throughout the field test. The temperature gradient data represents the gradient from the surface

to 3 meters. Most gradients are clustered between -2 to + 1 degrees, with most gradients being

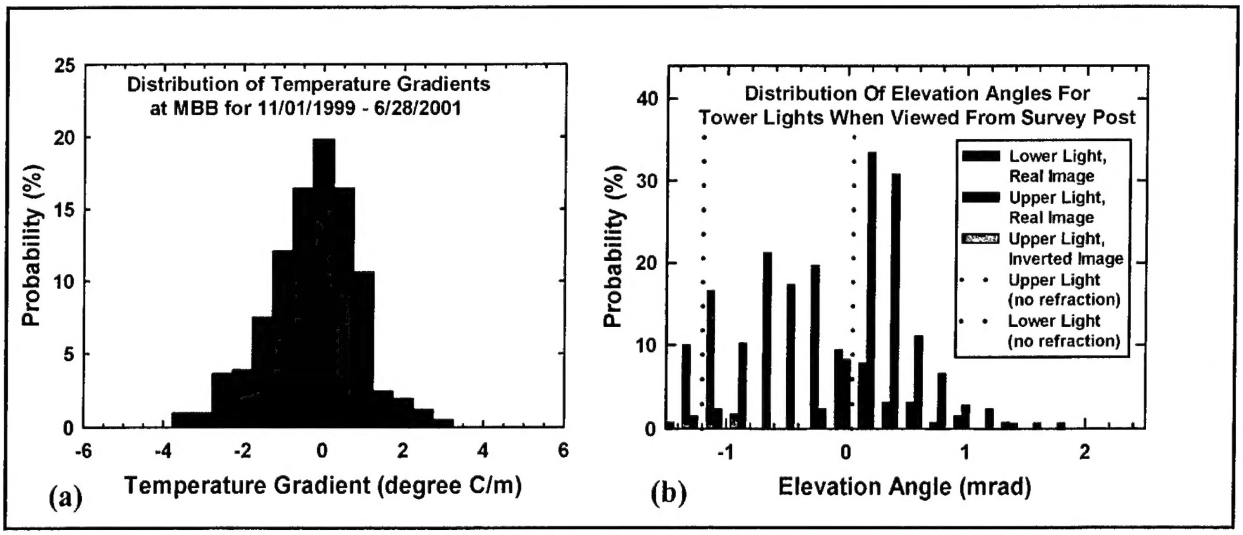

Figure 5

slightly negative. Only about 20 percent of the cases fall outside this range. Figure 5b shows the distribution of the apparent elevations of the upper (24.4 m) and lower (4.7 m) lights from the same time period as observed from the survey post (3.5 m). The upper light mainly appears at elevation angles between 0 and 1 mrad; during unstable conditions, an inverted image of the light appears between -1.5 and 1 mrad; and, during stable conditions, the lower light overlaps the range of the upper light. Note the probabilities for the lower light are less than 100% because the light is not visible during unstable conditions.

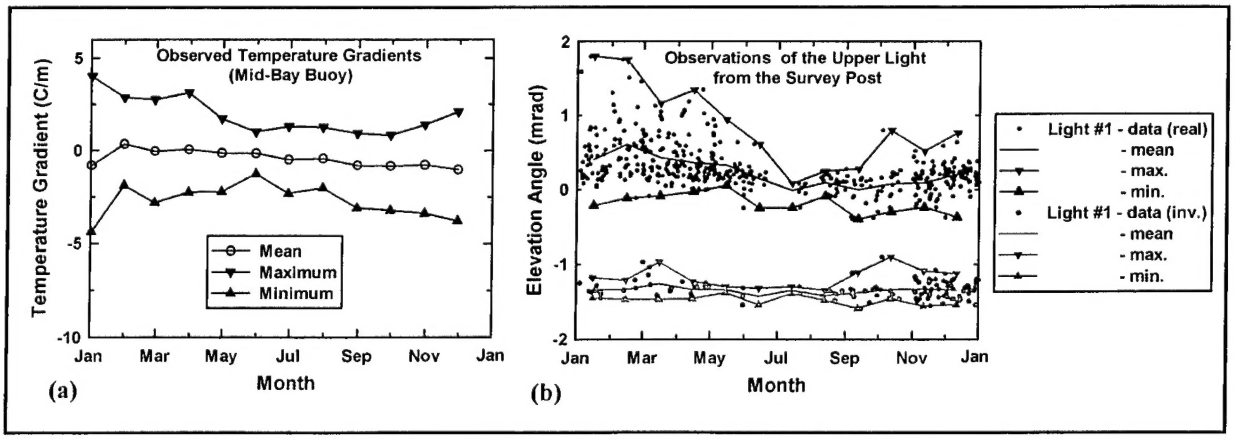

Figure 6

Figure 6a shows the monthly means of the temperature gradient, along with the minimums and maximums. The mean gradient decreases slightly over the year, from a slightly positive value in February, close to neutral in June and most negative in December. The extremes of the gradients occurred in January and the minimums in June. Although statistics have not been determined to see whether this behavior occurs routinely, it is logical to expect the greatest temperature extremes to occur in winter rather than in summer. This is the time when the water temperature is coldest and the air temperature varies widely. Figure 6b shows the annual variation of elevation angles for the upper light. The largest variation is in winter and the smallest is in summer. During winter, an image of the light can often be observe and images are rarely seen during the summer.

a. Survey Post Data

The first data examined is from the survey post, the second lowest site (where the height is 3.46 m). It is located at the bottom of the cliff and close to the water. This site was in use throughout the field experiment and was especially constructed for the program. It consisted of a stable concrete post with a platform on top on which to mount the survey station, see figure 3. This provided a site from which consistent and reliable data could be obtained.

Figure 7 shows the elevation angles of the upper light versus temperature gradient. The figure includes data from both the early morning and mid-day periods. A curve has been fitted to the data to show the trend. The elevation angle of the light is nearly constant for unstable conditions, increasing as the temperature gradient goes from negative to positive. The reason for the constant angle for negative gradients is unknown. The increasing angle with positive gradients is due to the decreased downward bending under stable conditions.

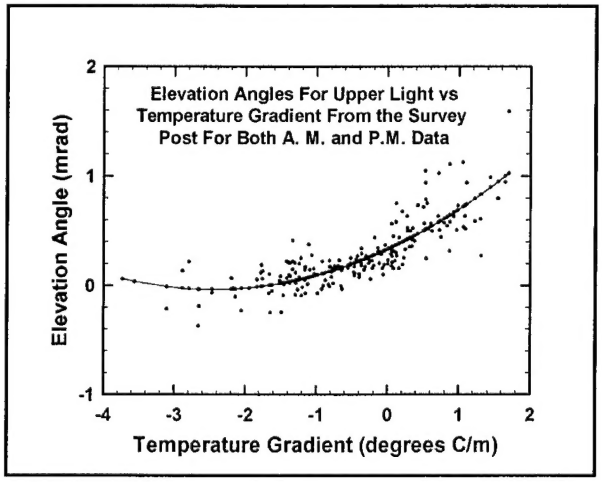

Figure 7

Somewhat surprising is the increased variability of the light's position during stable conditions, i.e. during positive gradients. This behavior is unexpected, since the lights are considered "better behaved" during stable conditions, being smaller in diameter and steadier in position.

To determine the reason for this behavior, several possible explanations were considered. First, water temperature differences between the two ground-truth sites were investigated. Large differences between sites could indicate non-uniform conditions along the path, making the mid-bay buoy site unrepresentative of the actual conditions. To this end, only data when the water temperatures were within one degree of each other were considered. This eliminated about thirty percent of the points, mainly unstable cases. However, eliminating these points failed to have any measurable influence on the scatter of the points for stable conditions.

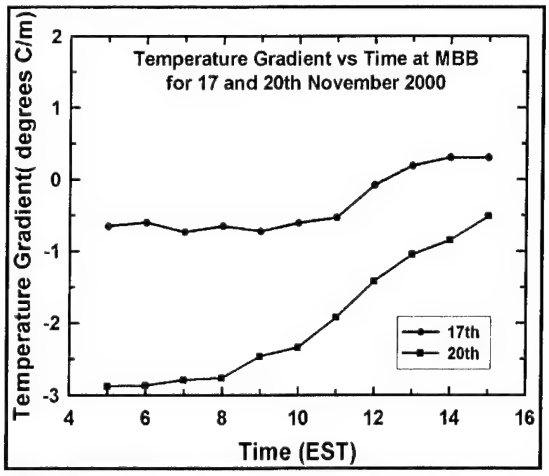

Figure 8

The next thought was to look at the temporal variations of temperature. In general, it is reasonable to expect temperatures would be more uniform across the Bay during the early morning hours, before the sun rose, than during mid-day, when land-sea breezes would occur. Examples of this behavior are shown in Figure 8, which shows two temperature time-histories taken during November 1999. In both cases, the water temperatures (not shown) were steady, while the air temperatures increased. However, in both cases, the temperatures were steady until after sunrise and changed rapidly during mid-day. Although Figure 8 is a time-history plot at a single location, one can easily make a case that this plot could represent the spatial distribution of temperatures across the Bay. However, after examining the time-histories of air temperature for a sampling of the scattered points, no correlation was found between the scattered points and days on which large temperature variations occurred.

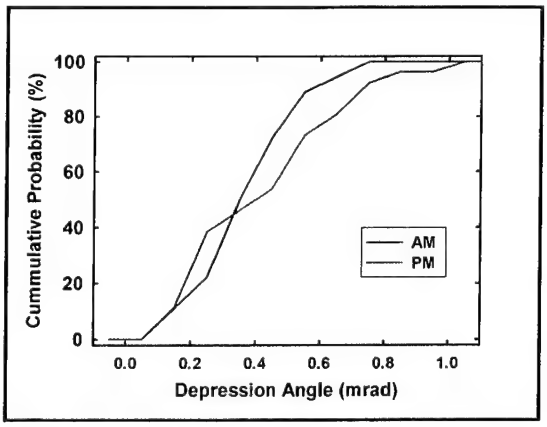

Figure 9

To see if separating the early morning and mid-day data affected the variability, Figure 9 shows the early morning data and mid-day data. The variability is much less for the early morning data. The question is why does this data show less variability, i.e. is " better behaved " then the mid-day data?

To answer this question, vertical temperature profiles were constructed by combining the two sources of ground-truth. The mid-bay buoy data was used to characterize the lowest layer, with the sea temperature equivalent to the surface temperature and the air temperature representing the temperature at a height of 3 meters. These data were combined with the air temperatures from Thomas Point Lighthouse at a height of 17.4 meters to create profiles between the surface and roughly 20 meters.

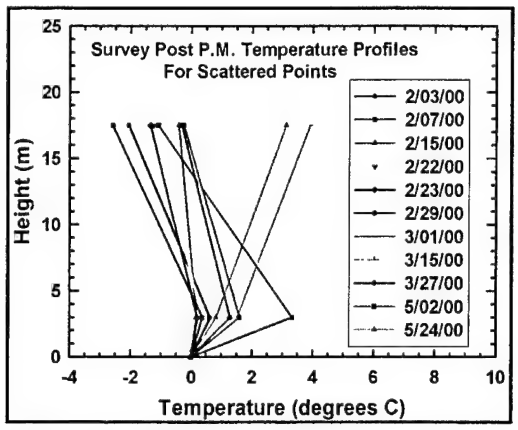

Figure 10

Since the mid-day data set had more scatter, profiles of these scattered points were compared to profiles of points closer to the curve fit. The data was restricted further to points with positive stability. Figure 10 shows the profiles from the scattered points. Nine of the eleven profiles are negative in the upper layer. Since all of the scattered points shown in Fig. 10 showed decreased bending, one would initially expect the profiles to be stable in the upper layer, rather than negative. However, the profiles suggest another explanation. Since the profiles are stable in the lower section and unstable above, the exact depth of the stable layer is unknown, only that it lies somewhere between 3 and 17.4 m. If it is deeper than 3 meters, the amount of bending would decrease even more, resulting in better agreement with the observed data. Figure 11 shows the profiles for the points that are closer to the curve fit. These cases are neutral in the upper layer, implying the stable layer is closer in depth to 3 meters.

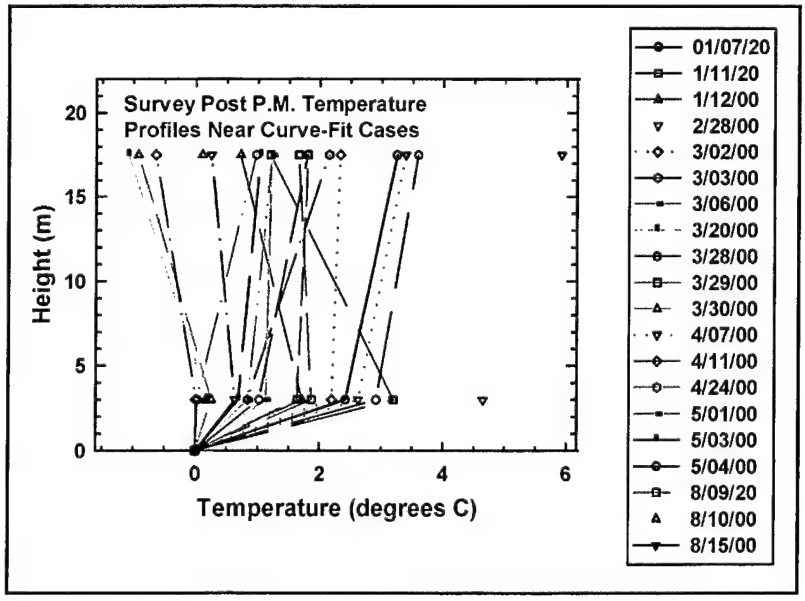

Figure 11

The early morning cases, although fewer in number, were also examined. The profiles for the points near to the curve again were neutral while the scattered points were mixed, with some being unstable and others stable.

One additional factor possibly influencing the observed scatter of the light's location during stable conditions is the presence of layers in the lower atmosphere. Under the proper conditions, they are the home of gravity waves, which are a well-known and studied phenomena. If present, these waves can cause changes in the location of the lights by changing the gradient. In the absence of gravity waves themselves, a stable layer can be tilted, again varying the location of the lights.

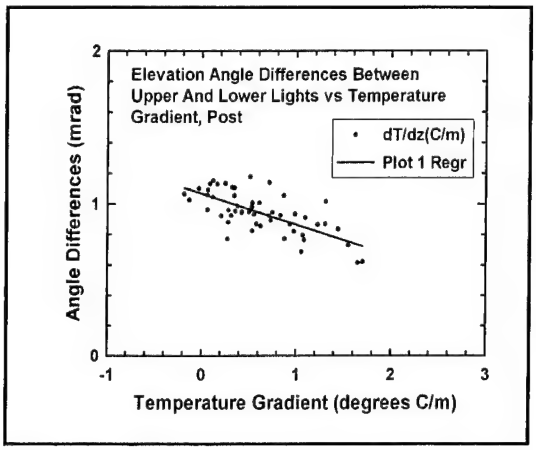

Figure 12

Figure 12 shows the separation between the upper and lower lights. The rays are not only bent less toward the earth as the gradient becomes positive, but are compressed together. Conversely, as the gradient becomes unstable, features are stretched vertically.

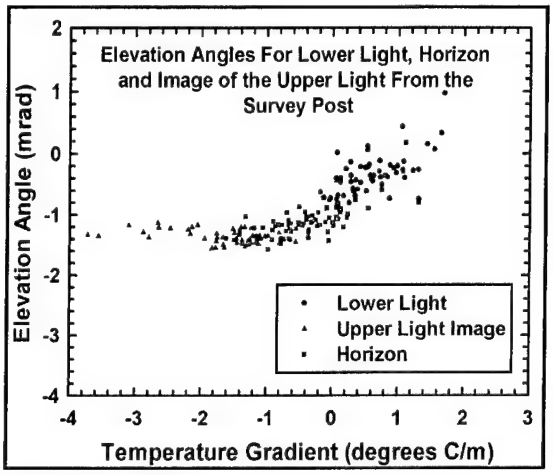

Figure 13

Figure 13 shows the elevation angles to the lower light, combined with the angles when the horizon and images were observed. Figure 13 includes both early morning and mid-day data. The curve shows the same general features as the upper light, including a steep rise for positive gradients. This steep increase is greater than the corresponding increase for the upper light because the lower light is affected more by the stronger gradients present at low altitudes. Interestingly, from the height of the survey post, the lowest light is observed only under positive stability, the horizon from slightly negative to neutral conditions, and images for strongly negative to neutral stability. The higher lights, being less influenced by the strong temperature gradient close to the surface, are visible during both unstable and stable conditions.

b. Building Data

Figure 14 shows the observed elevation angles versus temperature gradient for both the upper and lower lights from the highest site. This site, hgt = 37 m, was located in a room on the second story of a building on top of the cliff, Building 2 at CBD. The figure includes data from both the early morning and mid-day periods. From this height, no horizon or images were ever observed. For very unstable conditions, there is very little change in angle with temperature gradient, similar to the behavior observed from the lower site. As the atmosphere becomes stable, the position of the lights increase in height, but much more slowly than for the lower site. Also similar to the lower site is the increased variability in elevation angle for positive stabilities.

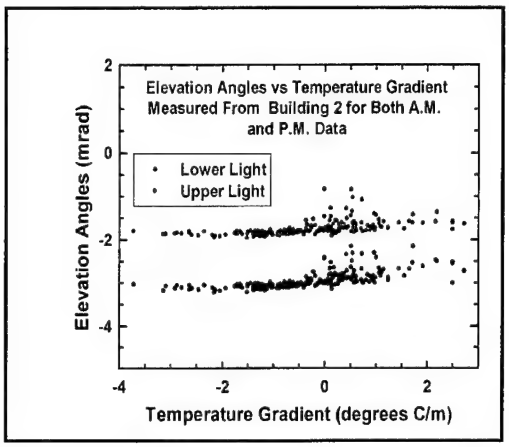

Figure 14

The data were separated again into early morning and mid-day groups, with slightly more scattered cases observed mid-day than early morning. Similar to the previous data, profiles of points close to a fitted curve were compared to those farther away. The results are summarized in Figure 15. Although the profiles showed individual variations, their averages showed distinct differences. The average profile for the data points close to the curve-fit was stable in the lowest layer and unstable above, while the scattered points were associated with stronger stability in the lowest layer and stable above. These stable profiles would produce upward bending not indicated by the measured gradient from 0 to 3 meters, thereby resulting in the scattered points.

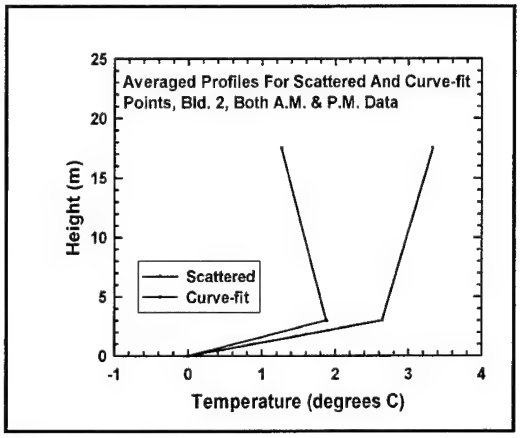

Figure 15

The separation between upper and lower lights are shown in Fig. 16. There is a slight decrease

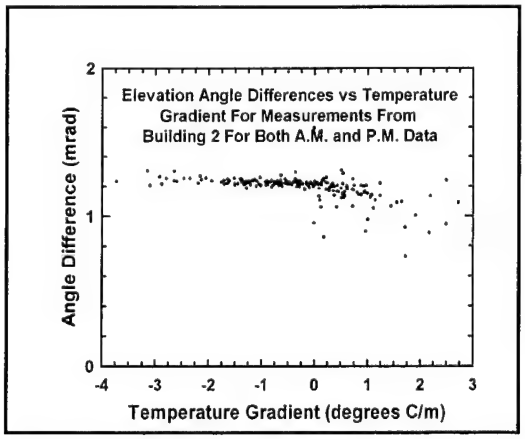

Figure 16

in angle as the stability becomes positive, i.e. a slight compression between rays, similar to the lower site data. The separation between the lights shows considerable variability as the gradient becomes positive, again consistent with results from the lower site. Eliminating the scattered points in Fig. 14 removes most of the scattered points in Fig. 16, but not all of them. The reason is unknown.

Some contamination of the data from this site was observed. During strong temperature differences between the building and outside air, the position of the lights would fluctuate rapidly, similar to turbulence. This behavior was controlled by using the average of five individual measurements. However, it raised the possibility that small angle errors were introduced by temperature differences between the building and the outside air.

To investigate this behavior further, angle measurements were made from this position to a target near the end of the pier and then reversed. If conditions were uniform, the angle magnitudes from the horizontal should be the same. However, a small difference was observed, indicating some effect of the building or the cliff on the observations. Although an effect was observed, it is unclear whether the presence of the building or cliff influenced the measurements in any detectable way. The observed scattered points were not correlated with days in which large temperature differences existed between the building and outside air.

c. Buoy Data

In addition to the data from lights at a fixed range, the range dependence of refractivity was investigated using six buoys located at ranges from 0.5 km to 4.0 km. Measurements of the azimuth and depression angles to the buoys were made at the same time each day as the tower lights from the various survey points.

The buoys were two foot diameter foam spheres painted bright orange to increase their visibility. They were tethered in place using a combination of ropes and chains attached to concrete anchors. They were placed either side of a straight line between CBD and Tilghman Island, increasing slightly in angle as the range increased. This made it easier to distinguish the buoys under poor visibility conditions. Because wave action made it difficult to accurately measure the angle to the water line at the buoy, the angles to the top of the buoys were measured instead. The height of this point above the water surface was determined from angle measurements between the water and the top of the buoy (0.43 m above the water surface). This was done on a calm day for the closest buoy.

The ranges to the buoys were determined by measuring the azimuth angles to the buoys from two separate locations, 400 meters apart, along the shoreline. Measuring the distance accurately between sites and the azimuth angles to the buoys from each site, the ranges were calculated using simple geometry. Since the buoys moved around on their tethers because of winds, currents and tidal flow, these measurements were repeated several times to obtain an average value, The same technique was used to verify the exact range to Tilghman Island tower. Midway through the investigation, these measurements were repeated because of a storm that re-positioned the buoys.

Table 1: Range to Buoys

Buoy #	Range (m) before storm	Range (m) after storm
1	694	685
2	1425	1414
3	2052	2020
4	2760	2707
5	3445	3440
6	4075	4104

Table 1 lists the measured ranges from the survey station, both before and after the storm. The change in position was not uniform for all buoys, ranging from a minimum of 5 m for buoy # 5 to a maximum of 53 m for buoy # 4.

Figure 17 shows the observed azimuth and elevation angles for all six buoys from the lowest site. Each buoy is clustered within about a 0.5 degree in azimuth and less than a 0.1 degree in elevation. Figure 18 shows the equivalent variation in meters for buoy # 1. It shows a 12 meters variation in azimuth and a one meter change in height. For buoy # 5 (see Fig. 19), the azimuth variation is 25 meters with a 3.5 meter change in height. Most of the height variations for buoy # 1 are due to changes in water height caused by tidal flow (see below). However, the variations in height from buoy # 5 are more likely due to refractive effects.

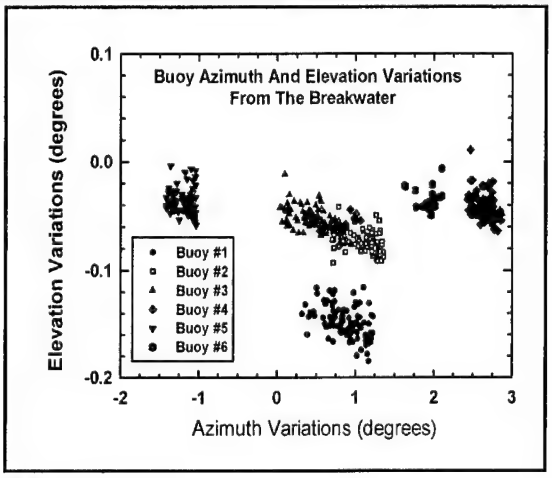

Figure 17

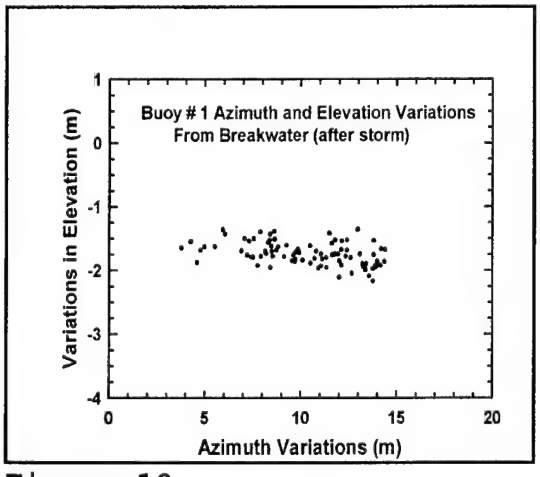

Figure 18

Water Level Variations

During the last part of the field measurements, estimates of water level relative to the survey sites were obtained at the same time as the optical and buoy measurements. A surveyors pole was used to note the water depth beneath the deck of the pier. Knowing the distance between the survey sites and the end of the pier and measuring the height difference between the survey sites and the pier deck, a reasonable estimate of water levels relative to each site could be determined.

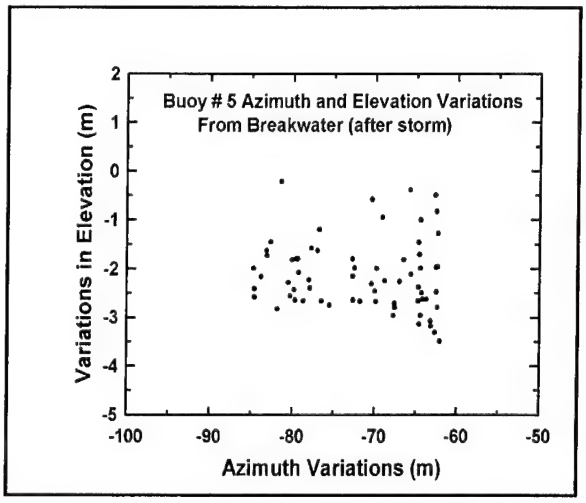

Figure 19

Figure 20 shows a histogram of the observed water levels below the deck of the pier. The height accuracy is estimated at seven centimeters, since the heights were estimated from averages of the wave crests and troughs. These heights were compared to the water heights derived from #1 buoy data obtained from the breakwater. Figure 21 compares the observed water heights versus the heights derived from the elevation angles measurements. The buoy data have been corrected for the height of the buoy above the water line and the earth's curvature. The correlation is good, indicating the fluctuations in elevation angle at buoy # 1 are primarily due to changes in water height.

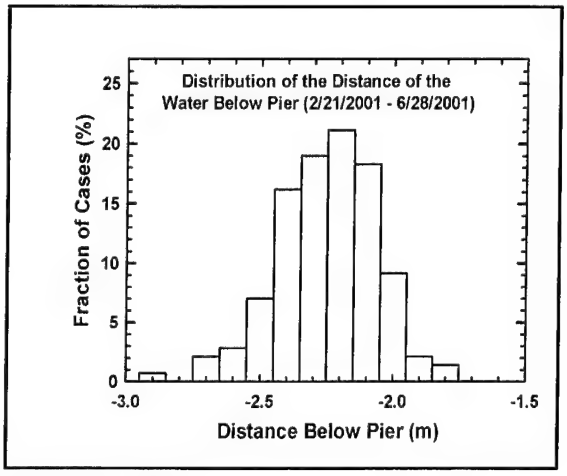

Figure 20

Refractive Effects

The range dependence of refractivity was investigated by comparing the observed buoy elevation angles, corrected for buoy height above the water line, to the angles calculated from the observed water height and buoy ranges. This last angle is without any atmospheric influence, but is corrected for the earth's curvature.

Figure 22 shows the results for buoy #1. The average is close to zero between the observed and calculated values for all observed gradients. This result is to be expected, as there only was a short path through the atmosphere to buoy #1.

As the path length increases, the downward bending increases for unstable conditions (see Fig. 23). As the conditions becomes stable, the amount of downward bending decreases, eventually reversing and bending upwards as the gradient becomes positive. This shape of the data is similar to the results from the tower lights observed from the same position (see Fig. 13). Buoy # 5 data were used because there were insufficient data from buoy #6.

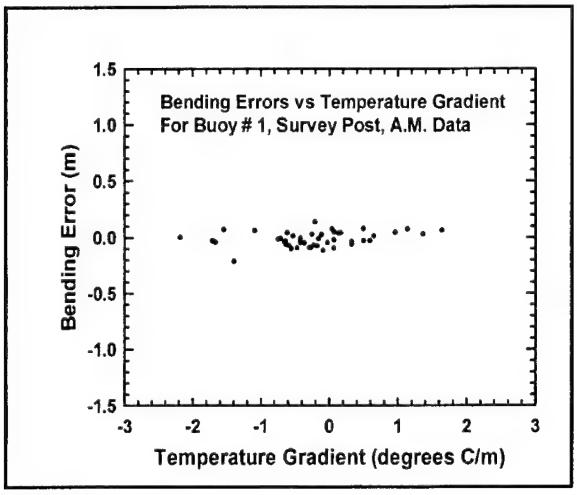

Figure 22

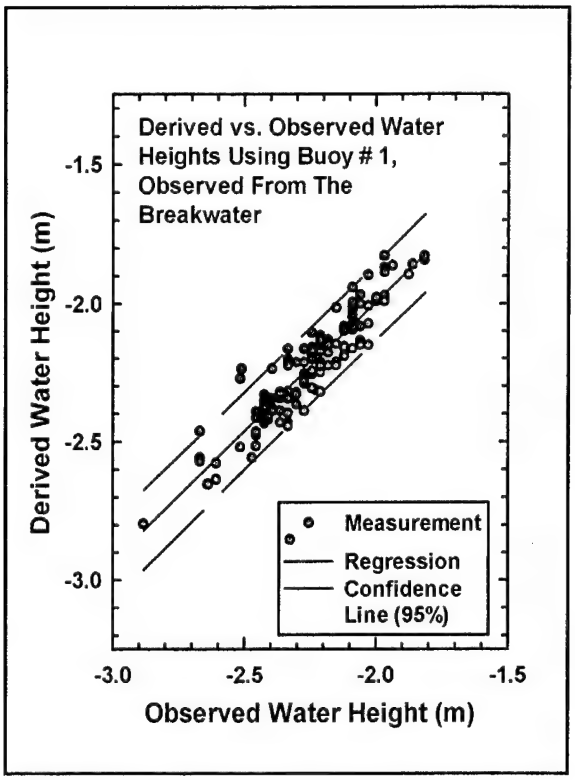

Figure 21

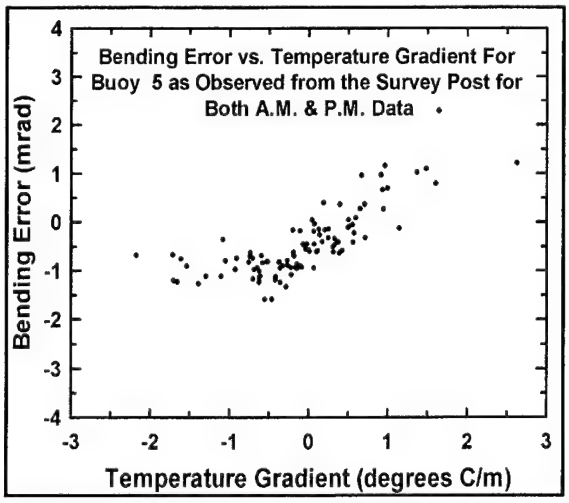

Figure 23

d. Refractive Model

Using the observed elevation of targets and observed air-sea temperature differences, we derive a non-dimensional relationship between the elevation and the temperature differences. The general utility of the model is unknown as it is only based on observations of the Chesapeake

Bay.

If the surface layer has a constant lapse rate, optical rays passing through the layer follow a constant trajectory with a constant curvature (Lehn, 1983):

$$z = -\frac{x^2}{2r_o} + x \tan \theta_o + z_o, \qquad (1)$$

where z is height above the surface, x is the horizontal range, r_o is the radius of curvature, θ_o is the initial elevation angle, and z_o is the height of the observer. The curvature is:

$$\frac{1}{r_o} = \frac{\varepsilon \rho}{(1 + \varepsilon \rho)T} \left(\frac{dT}{dz} + g \beta \right) \qquad (2)$$

where ρ is the density of air, ε is 2.26 x 10-4 from the refractive index of air ($n=1 + \varepsilon \rho$), g is the acceleration of gravity and β is 3.48e-3, the reciprocal of the specific gas constant.

The curvature of an observed ray can be estimated from the difference between the measured elevation angle (θ_o), the elevation that the target would appear at if there was no refraction (θ_t), and the range to the target (x_t):

$$\frac{1}{r} = \frac{2(\theta_o - \theta_t)}{x_t} \qquad (3)$$

The measured curvature is scaled by the curvature of a ray in a neutral atmosphere ($1/r_n$) providing a non-dimensional number, κ, which will be called the normalized curvature:

$$\kappa = \frac{r_n}{r} - 1, \qquad (4)$$

where r_n is:

$$\frac{1}{r_n} = \frac{\varepsilon \rho g \beta}{(1 + \varepsilon \rho)T} \qquad (5)$$

and has a numerical value of 29334.1 km.

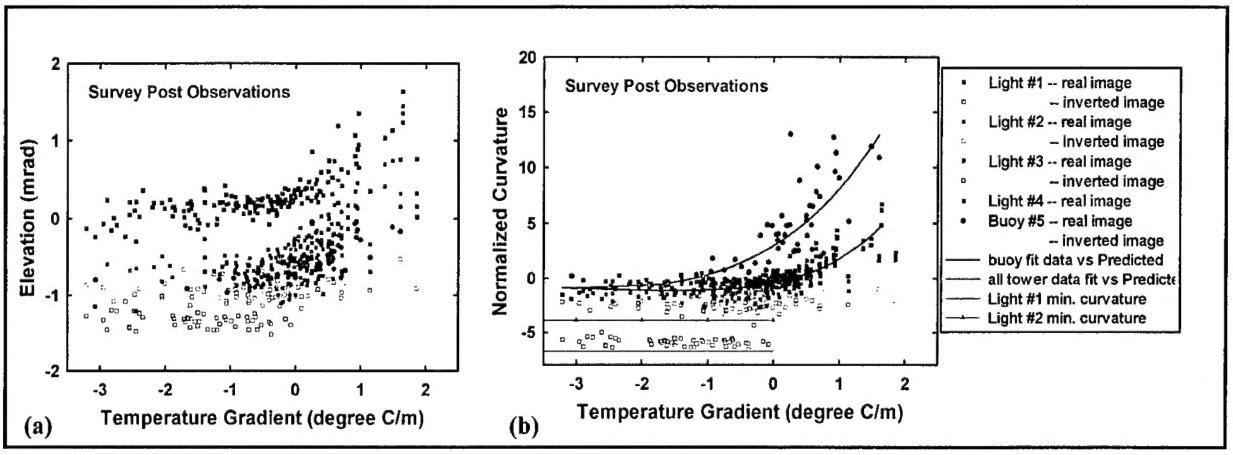

Figure 24

Figure 24a shows the elevation angle observed for the tower lights and buoy #5. Using the normalized curvature reduces the vertical variation for the tower lights, see figure 24 b. This figure shows the non-dimensional number (k) for the tower lights as observed from the survey post at a height of 3.5 meters and the results for buoy # 5 from a height of 2.3 m. An exponential curve was fit to the data from the tower lights and found that there was no significant difference between the curves. Instead, we fit a single exponential curve to all the tower data:

$$\kappa_f = (a_1 \Delta + a_2) \exp[a_3 \Delta + a_4] + a_5 \qquad (6)$$

where κ_f is the fitted curvature, Δ is the temperature gradient, and the parameters for the tower fit are 0.85, -0.28, 0.54, 0.55, and 0.0063. A similar curve was fit to the buoy #5 data where the fit parameters are 1.35, -1.13, 0.28, 1.28, and 7.05; however, the buoy data differs significantly from the tower data. This difference is probably caused by the different trajectories; the buoy trajectories are lower and shorter than the tower trajectories. The buoy data has a larger variation than for the tower data; in part, this variation is caused by changes in the water level (caused both by tide and waves), which introduces a height error not present in the tower data. Data from

buoy #5 observed from the survey post and data from buoy #6 for both the survey post and breakwater yield curves similar to the plotted buoy #5 data observed from the breakwater.

The inverted images are caused by rays that bend up near the surface where the temperature gradients are the largest. The smallest curvatures, κ_m observed can be estimated by driving the curvature of the rays that skim just above the water surface:

$$\kappa_m = -\frac{r_n}{r_e} - \frac{2\, r_n\, (z_t + z_o) + 4\, r_n \sqrt{z_t\, z_o}}{x_o^2} \qquad (7)$$

where z_t and z_o are the heights of the light and survey station respectively, x_o is the distance between the survey station and light, and r_e is the radius of the Earth. Figure 24b shows the smallest curvatures (or min. curvature in the graph's legend) are just below the curvatures measured for the images.

4. SUMMARY AND CONCLUSIONS

Optical refraction can be used as an indicator of atmospheric stability. Viewed across an uniform body of water, the position of lights arranged vertically on a tower can be used to determine atmospheric conditions close to the water surface. The number of lights observed, their spacing, whether the horizon or images are observed indicates stable, near neutral or unstable atmospheric conditions respectively. The effects are strongly dependent on observer height, so the effects are best seen at low altitudes (hgt < 10 m).

For stable conditions, the rays are bent downward less than normal, making the lights appear at higher elevation angles. This allows one to see beyond the normal horizon and allows observation of lights located at low altitude. In addition, the separation between lights decreases, i. e. features are compressed together. An unexpected behavior uncovered during stable conditions is the increased variability of the light's position. Investigation indicated that it is not caused by temporal variations in temperature or to non-homogeneous conditions across the path. It could be the use of the temperature gradient between the surface and 3 meters to describe the atmospheric stability. This parameter doesn't accurately indicate the depth of the stable layer, missing depths between 3 to 17.5 m. Deeper stable layers would produce more upward bending, consistent with the observed results. One additional situation that occurs during stable conditions is the presence of gravity waves. Their fluctuations could cause the lights to appear

and disappear, drift in elevation and lose sharpness. It is unknown whether or how much they were responsible for the variability.

For temperature gradients close to neutral, the rays are bent more toward the earth's surface, striking the water before they reach the lowest light. Therefore, the bottom light is missing, leaving only the top light(s), along with the horizon (the water). As the temperature gradient becomes negative, an image of the upper light appears whose position approaches a plateau as the gradient becomes more negative. As noted earlier, this is because there are two paths to the lights, a direct path and one that skims the water surface and then rises to the light. The path that skims the surface makes the light appear below the astronomical horizon. The reason for the image positions becoming constant with negative stability is unknown. These same results occur as the height of the observer increases, only to a smaller extent. However, for the highest observer height, (hgt = 37 m), the horizon and images were not observed.

The range dependence of refraction was investigated using the change in elevation angle of six buoys placed from 0.5 to 4 km away from the site. The results agreed with the results observed from the lights at a fixed range. The bending decreases at the temperature gradient becomes less negative, bending upwards as the gradient becomes positive. Additionally, the amount of bending increases as the path length increases.

There is a seasonal trend to these results, with more unstable conditions in the fall and stable conditions in the spring. The most typical gradient is slightly negative.

A normalized curvature can be calculated and this process reduced variability of the tower data; however, the normalization did not appear to reduce the buoy data. The variation in the buoy data is caused by both refraction and water level variations. It may be necessary to use short range buoy data to remove water level variations before normalizing the curvature. We did not have access to high quality turbulence data, which could be useful in characterizing the depth and shape of the surface layer. Using a non-dimensional temperature gradient reduces the errors in the fit between the normalized curvature and the temperature gradient; making the curve useful universally.

Remote refractivity measurements can quickly and easily characterize the near-surface temperature field over uniform bodies of water or ice. It has the advantage of providing data over a path rather than the point measurements obtain by in situ sensors. In addition, this technique is not troubled by harsh marine environments, which can quickly deteriorate standard sensors. Disadvantages include the necessity of good visibility to see the target and uniform meteorological condition between sites.

REFERENCES

1. J. C. Johnson, *Physical Meteorology,* The M.I.T. Press,(1954).

2. R. G. Fleagle and J. A. Businger, *An Introduction to Atmospheric Physics*, 2nd ed. Academic Press, New York,(1980).

3. R. G. Fleagle, "The Optical Measurement of Lapse Rate", Bull. Am. Meteorol. Soc., **31,** 51-55, (1950).

4. A. B. Frazer, "Simple solution for obtaining a temperature profile from the inferior image", Appl. Opt. **18,** 1724-1731, (1979).

5. W. H. Mach and A. B. Frazer, "Inversion of optical data to obtain a micrometeorological temperature profile", Appl. Opt. **18**, 1715-1723,(1979).

6. W. H. Lehn, "Inversion of superior mirage data to compute temperature profiles", J. Opt. Soc. Am., **73**, # 12, 1622-1625,(1983).

7. W. P. Hooper, G. Nedoluha, and L. U. Martin, "Retrieval of near-surface temperatures profiles from passive and active optical measurements," Opt. Eng. (accepted for publication in July 2002).